J Biochem 130, 679–686 (2001)

Mechanism of Chitosanase–Oligosaccharide Interaction: Subsite Structure of *Streptomyces* sp. N174 Chitosanase and the Role of Asp57 Carboxylate[1]

Hugo Tremblay,* Tsugihisa Yamaguchi,† Tamo Fukamizo,† and Ryszard Brzezinski*,[2]

**Centre d'Étude et de Valorisation de la Diversité Microbienne, Département de Biologie, Faculté des Sciences, Université de Sherbrooke, 2500 Boul. de l'Université, Sherbrooke (Quebec) J1K 2R1 Canada, and* †*Laboratory of Enzyme System Science, Department of Food and Nutrition, Kinki University, 3327-204 Nakamachi, Nara 631-8505*

Received June 26, 2001, accepted September 4, 2001

We have investigated the mechanism of the interaction of *Streptomyces* sp. N174 chitosanase with glucosamine hexasaccharide [$(GlcN)_6$] by site-directed mutagenesis, thermal unfolding, and $(GlcN)_6$ digestion experiments, followed by theoretical calculations. From the energy-minimized model of the chitosanase-$(GlcN)_6$ complex structure (Marcotte *et al.*, 1996), Asp57, which is present in all known chitosanases, was proposed to be one of the amino acid residues that interacts with the oligosaccharide substrate. The chitosanase gene was mutated at Asp57 to Asn (D57N) and Ala (D57A), and the relative activities of the mutated chitosanases were found to be 72 and 0.5% of that of the wild type, respectively. The increase in the transition temperature of thermal unfolding (T_m), usually observed upon the addition of $(GlcN)_n$ to chitosanase mutants unaffected in terms of substrate binding, was considerably suppressed in the D57A mutant. These data suggest that Asp57 is important for substrate binding. The experimental time-courses of [$(GlcN)_6$] degradation were analyzed by a theoretical model in order to obtain the binding free energy values of the individual subsites of the chitosanases. A (–3, –2, –1, +1, +2, +3) subsite model agreed best with the experimental data. This analysis also indicated that the mutation of Asp57 affects substrate affinity at subsite (–2), suggesting that Asp57 most likely participates in the substrate binding at this subsite.

Key words: chitooligosaccharide, chitosanase, subsite, substrate binding, unfolding.

Chitosanase is a member of the glycoside hydrolase family of enzymes and is characterized by its ability to catalyze the hydrolytic cleavage of chitosan, a polycationic carbohydrate derived from chitin by partial or complete deacetylation. Chitosan is a mixed polysaccharide containing β-1,4-linked residues of β-D-glucosamine (GlcN) and *N*-acetyl-β-D-glucosamine (GlcNAc). The relative amounts of these two monomers in chitosans vary depending on their source. Most chitosans contain 20 to 35% GlcNAc. The GlcNAc content in chitosan is also described as the degree of *N*-acetylation (d.a.) of chitosan. In contrast to chitin, chitosans with various d.a.'s are soluble in aqueous buffers at moderately acidic pH, rendering these polymers much more amenable to enzymatic hydrolysis. Chitosan has been used as a substrate in many enzymatic studies, not only with chitosanases but also with chitinases, lysozymes, and several other classes of hydrolytic enzymes. It became immediately apparent that the various categories of enzymes have different preferences with respect to the d.a. of chitosan. Lysozymes and chitinases are more active against chitosans with high d.a., while chitosanases preferably attack chitosans with low d.a. However, as the physical properties of chitosan vary widely with changes in the d.a., the relationship between enzymatic activity and chitosan d.a. could not be used to characterize the various categories of enzymes.

Further elucidation of the differences in the mechanisms of chitosan hydrolysis among various groups of enzymes came from experiments that analyzed the structure (*i.e.* the sequence) of the oligosaccharide products of hydrolysis. From these sequences, the cleavage specificity of several enzymes could be deduced. Fukamizo *et al.* (*1*) proposed classifying chitosanases as enzymes that hydrolyze chitosan without splitting the linkage GlcNAc-GlcNAc. Conversely, chitinases cleave the GlcNAc-GlcNAc linkage, but not the GlcN-GlcN linkage. Chitosanases were further subdivided into three classes according to their cleavage specificity; class I enzymes split both GlcN-GlcN and GlcNAc-GlcN linkages; class II enzymes split only GlcN-GlcN linkages; and class III enzymes split both GlcN-GlcN and GlcN-GlcNAc linkages. Subsequent work on chitinases (*2, 3*) showed that they can also be divided into at least two subclasses; the chitinase from *Bacillus circulans*, which can cleave both GlcNAc-GlcNAc and GlcNAc-GlcN linkages;

[1] This work was supported by research grants from the Natural Sciences and Engineering Research Council of Canada to R.B. and from the Elizabeth Arnold Foundation, Japan, to T.F.

[2] To whom correspondence should be addressed. Tel. +1-819-821-8000 (Ext. 1077), Fax: +1-819-821-8049, E-mail: rbrzezin@courrier.usherb.ca, WWW page: http://callisto.si.usherb.ca/~rbrzezin/index

Abbreviations: GlcN, 2-amino-2-deoxy-D-glucopyranose; GlcNAc, 2-acetamido-2-deoxy-D-glucopyranose; $(GlcN)_n$, β-1,4-linked oligosaccharide of GlcN with a polymerization degree of *n*; d.a., degree of acetylation; N174 chitosanase, chitosanase from *Streptomyces* sp. N174; HEWL, hen egg white lysozyme.

and, the chitinase from *Streptomyces griseus* HUT 6037, which cleaves GlcNAc-GlcNAc and GlcN-GlcNAc linkages. Finally, a detailed study of the cleavage specificity of HEWL (*4*) showed that this enzyme has a strong preference for the cleavage of GlcNAc-GlcNAc linkages, but that it is also able to cleave GlcN-GlcNAc linkages. The recognition mechanisms of the chitinolytic enzymes are thus complicated, making it difficult to distinguish unequivocally between these enzymes.

Our long-term goal is to understand the substrate recognition mechanism of chitinolytic enzymes, particularly the chitosanase from *Streptomyces* sp. N174. This enzyme belongs to class I chitosanases (*1*), and its properties have been reviewed (*5*) Its catalytic residues and three-dimensional structure have been determined (*6, 7*). Several experimental findings indicate that carboxylic amino acid residues may play an important role in determining both the mode of substrate binding and the cleavage specificity of this chitosanase. At least 12 carboxylic residues are found in the active site cleft of the chitosanase from *Streptomyces* sp. N174 (*7*) and could participate in the binding of the positively charged chitosan substrate in both specific and nonspecific ways. A model for the binding of glucosamine hexasaccharide, $(GlcN)_6$, to chitosanase has been proposed (*7*), adopting a (–4)(–3)(–2)(–1)(+1)(+2)-type enzyme-substrate interaction typical of hen egg white lysozyme (*8*). According to this model, four carboxylic residues could be directly involved in links with the substrate, promoting the binding of low d.a. chitosan by chitosanase These four residues are Glu60, Asp57, Glu197, and Asp201, and localize at subsites (–4), (–2), (–1), and (+2), respectively. The first three of these residues could form ion pairs with the amino groups of the substrate. Asp57 could also form a hydrogen bond with an O3 group of the sugar at subsite (–2).

In this report we investigate the chitosanase-oligosaccharide interaction using wild type and Asp57-mutated chitosanases from *Streptomyces* sp N174, and discuss the role of Asp57 in the enzyme-substrate interaction. We also present an alternative model of subsite arrangement in the active site cleft of the chitosanase based on the results of oligosaccharide hydrolysis experiments

MATERIALS AND METHODS

Materials—Glucosamine oligosaccharides [$(GlcN)_n$, n = 3–6] were obtained from Seikagaku Kogyo. Chitosan substrate (d.a., 0.21) used for preliminary enzyme assays during enzyme purification was purchased from Sigma. Chitosan with the lowest degree of acetylation and a lower degree of polymerization (d.a. <0.01; d.p. ≈20) used for thermal unfolding experiments was kindly donated by Dr. Vårum, Norwegian University of Science and Technology. Other reagents were of commercially available analytical grade.

Bacterial Strains and Plasmids—*Escherichia coli* strains JM109 (*end*A1, *thi*, *gyr*A96, *hsd*R17(rk⁻, mk⁻), *rel*A1, *sup*E44, D(*lac-pro*AB),[F′, *tra*D36, *pro*AB, *lac*I^{q}zΔM15]) and BMH 71-18 (*thi*, *sup*E, Δ(*lac-pro*AB), [*mut*S::Tn10][F′, *pro*AB, *lac*I^{q}zΔM15]) were purchased from Promega (Madison, WI). *Streptomyces lividans* TK24 (*9*) was kindly provided by Dr. D.A. Hopwood. The vector pALTER-1 (for site-directed mutagenesis) and the shuttle vector pFD666 (used for the expression of wild type and mutated genes in *S. lividans*) was described previously (*6, 10*).

Site-Directed Mutagenesis—Mutations were introduced into the *csn* gene using the vector pALTER-1 carrying the wild type chitosanase gene (*6*) Mutations were created according to the Altered Sites procedure (Promega). The oligonucleotides used for the mutagenesis were 5′-TCCAGCATGTTGCCGGTCCCG-3′ for D57N, 5′-TTCCAGCATGGCGCCGGTCCC-3′ for D57A, and 5′-GAGGAGTTCTGGGCGCTGGAG for E22Q. All of the mutated genes were completely sequenced. The mutated genes were then excised by *Hin*dIII and *Xba*I digestion, subcloned in pFD666 vector, and transformed into *S. lividans* for expression.

Enzyme Production, Purification, and Assay—Wild-type and mutated chitosanases were produced and purified from *S. lividans* cultures (1.6 liters for each mutant) as previously described (*6, 11*). Chitosanase activity was determined using the reducing sugar assay (*12*). For standard activity assay, the chitosan substrate was dissolved at a final concentration of 0.8 mg/ml in 50 mM acetate buffer, pH 5.5, and then incubated with enzyme for 10 min at 37°C prior to terminating the reaction by the addition of the *p*-hydroxybenzoic acid reagent (*12*). Final yields of purified chitosanases were 85.2, 1.3, and 0.85 mg, respectively, for D57N, D57A, and E22Q mutants (established from the absorption at 280 nm using a coefficient of 30,300 M^{-1}) (*6*).

Thermal Unfolding Experiments—Thermal unfolding curves of chitosanases in either the presence or absence of $(GlcN)_n$ were obtained experimentally in 50 mM sodium phosphate buffer, pH 7.0, using a Jasco J-720 spectropolarimeter (cell length, 0.1 cm). The CD value at 222 nm was monitored while raising the temperature at a rate of 1°C per min. The temperature was measured using a DP-500 thermometer (Rikagaku Kogyo). The experimental data were normalized by linearly extrapolating the pre- and post-transition baselines into the transition zone and then plotting against temperature. Assuming that the unfolding equilibrium of the chitosanase follows a two-state mechanism, the unfolding curves were subjected to least squares analysis in order to obtain the midpoint temperatures (T_m) and the thermodynamic parameters. The enthalpy and entropy changes at T_m (ΔH_m and ΔS_m) were calculated using van't Hoff analysis The difference in the free energy change of unfolding (at T_m of the wild type protein) from that of the free protein ($\Delta\Delta G_m$) was estimated by the relationship, $\Delta\Delta G_m = \Delta T_m \cdot \Delta S_m$(free), where ΔT_m is the differ-

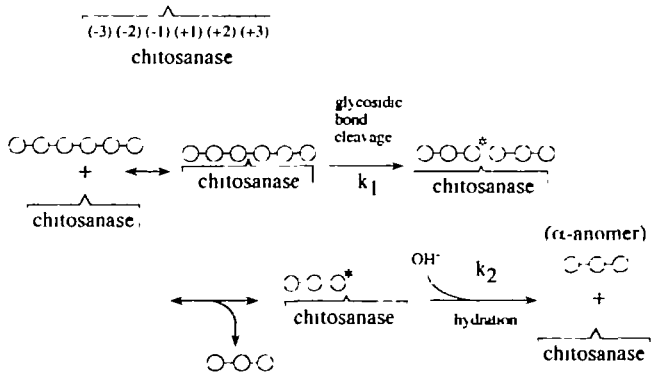

Fig. 1. **Theoretical reaction model of the chitosanase-catalyzed hydrolysis of glucosamine hexasaccharide.** In the calculations, all possible binding modes are taken into consideration

ence in T_m from that of the free protein and ΔS_m(free) is the entropy change of the free protein at T_m (*13*).

HPLC Determination of the Reaction Time-Course—The enzyme sample was added to $(GlcN)_6$ solution and the mixture was incubated in 50 mM sodium acetate buffer, pH 5.0, at 40°C. At various time points of the reaction, aliquots were removed and the reaction was quenched by the addition of an equal volume of 0.1 M NaOH. Substrate and product concentrations were determined by HPLC using a TSK-GEL G2000PW (Tosoh) gel filtration column (7.5 × 600 mm) connected to a differential refractometer (Hitachi L-3350). The elution was performed with 0.5 M NaCl at a flow rate of 0.3 ml/min at room temperature.

Theoretical Calculation of the Reaction Time-Course—Theoretical analysis of the reaction time-course was performed by the method described previously (*14*). The reaction model is shown in Fig. 1. Bond cleavage (k_1) and hydration (k_2) are assumed to be time-dependent, but all other steps are time-independent binding processes. Binding constants are defined for all possible binding modes, and were calculated from the unitary binding free energy changes of individual subsites by assuming the additivity of the free energy values. Having observed that trimeric products are preferentially generated from the hexameric substrate, and taking into account the structural similarity between barley chitinase and the chitosanase, we tested a model assuming that the chitosanase has a subsite arrangement similar to that of barley chitinase, specifically (–3)(–2)(–1)(+1)(+2)(+3). The value of the binding free energy change of each subsite was estimated using the optimization technique based on the modified Powell method (*15*) employing the cost function,

$$F = \sum_i \sum_n [(\mathrm{GlcN})^c_{n,i} - (\mathrm{GlcN})^e_{n,i}]^2$$

where e and c are the experimental and calculated values, n is the size of the oligosaccharide, and i the reaction time. In calculating the reaction time-course, the value of the rate constant k_1 (for cleavage of the glycosidic linkage) was assumed to be dependent on the size of the substrate, and the k_{cat} values obtained from the steady state kinetic analysis with oligosaccharide substrates, 50 s^{-1} for $(GlcN)_4$, 50 s^{-1} for $(GlcN)_5$, and 200 s^{-1} for $(GlcN)_6$ (Fukamizo *et al.*, unpublished data), were allocated to the individual k_1 values. As previously reported (*23*), N174 chitosanase catalysis takes place through an inverting mechanism, in which the hydration occurs almost concurrently with bond cleavage. Thus, the higher value, 1,000 s^{-1}, was tentatively allocated to k_2, the rate constant for hydration.

RESULTS

Choice of Residues for Mutagenesis—Asp57 was selected for site-directed mutagenesis studies for three reasons. First, comparison of the distribution of the electrostatic potential between the chitinase from barley seeds and the chitosanase from *Streptomyces* sp. N174 (Fig. 2) prompted the conclusion that the electronegative character of the active site cleft of the chitosanase is one of the factors that determines the difference in substrate preference between these two enzymes. Secondly, the model proposed by Marcotte *et al.* (*7*) suggested that Asp57 occupies a central position in the active site cleft of the N174 chitosanase, and this residue is observed to be conserved in all chitosanases belonging to family 46 of glycoside hydrolases (Fig. 3A). Thirdly, the structure-based alignment of this portion of the chitosanase sequence with the chitinase from barley seeds (*16*), which belongs to family 19, revealed that there is an asparagine residue in the chitinase in a position analogous to that of Asp57 in N174 chitosanase (Fig. 3B). This asparagine is strictly conserved in all chitinases belonging to family 19, and its mutation to alanine in barley chitinase results in a severe loss of activity (*17*) It was thus interesting to investigate in detail the function of the Asp57 residue of N174 chitosanase.

Enzymatic Activities of Asp57-Mutated Chitosanases toward Chitosan—We purified two mutated chitosanases, D57N and D57A, with the Asp57 residue replaced with Asn and Ala, respectively Both mutant chitosanases were found to retain most of their wild type global conformation as judged from CD spectroscopy. The enzymatic activities of both mutated chitosanases toward the $(GlcN)_6$ substrate were measured and compared with that of the wild type enzyme. The relative activities of mutants D57N and D57A were 72 and 0.48% of that of the wild type, respectively. Clearly, the mutation of Asp57 affects the enzymatic activity, especially the mutation to alanine. Steady state kinetic

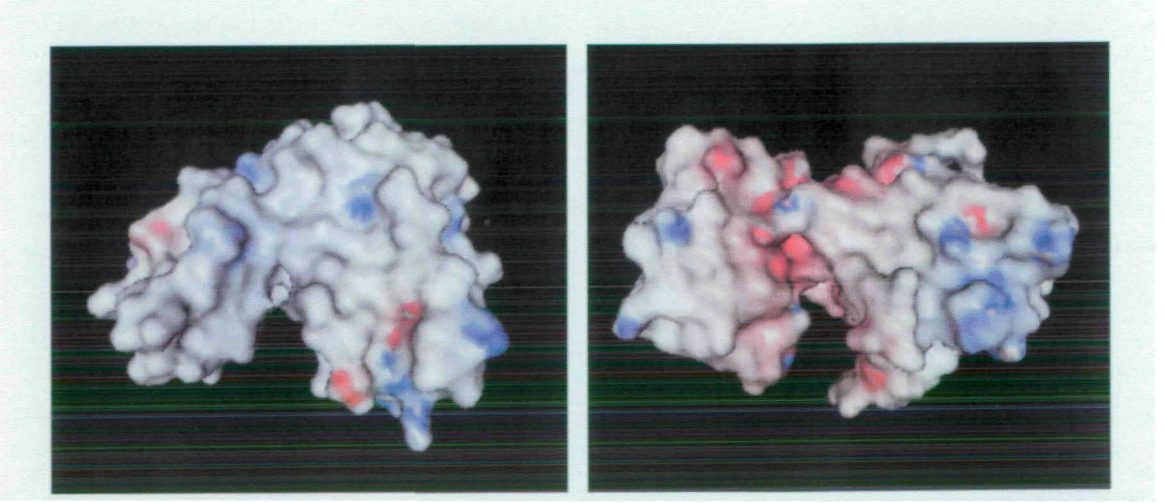

Fig 2 **Comparison of the density of charges at the surface of the chitinase from barley (left) and the chitosanase from *Streptomyces* sp. N174 (right).** The negative charges are in red, the positive charges in blue

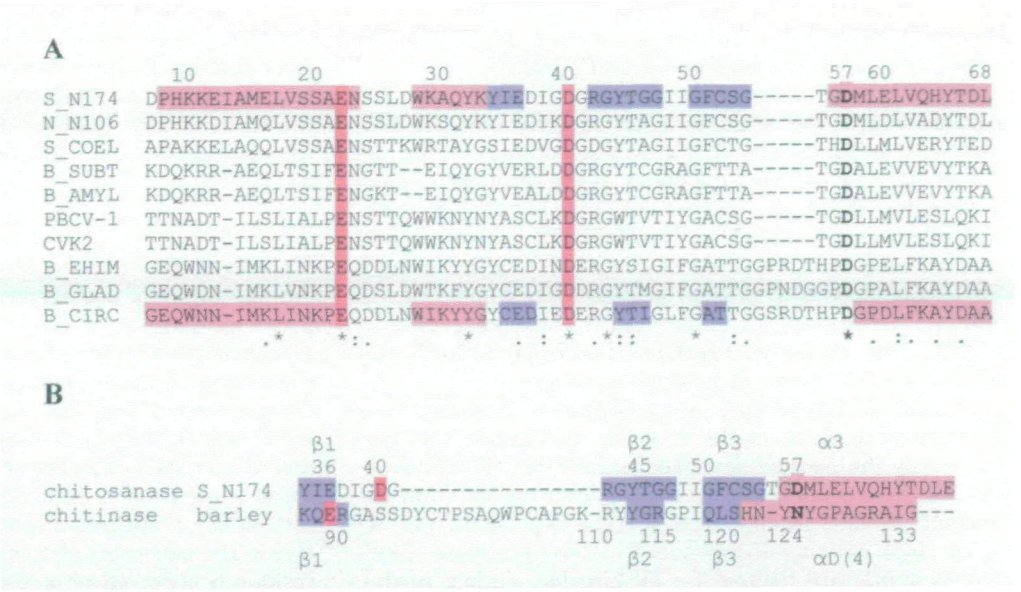

Fig 3 (A) Alignment of the highly conserved N-terminal modules from ten sequenced chitosanases belonging to glycoside hydrolase family 46. S_N174, *Streptomyces* sp N174, N_N106, *Nocardioides* sp N106, S_COEL, *Streptomyces coelicolor* A3(2); B_SUBT, *Bacillus subtilis*, B_AMYL, *Bacillus amyloliquefaciens*; PBCV_1, *Chlorella virus* PBCV-1, CVK2, *Chlorella virus* CVK2; B_EHIM, *Bacillus ehimensis*, B_GLAD, *Burkholderia gladioli*, B_CIRC, *Bacillus circulans* MH-K1 Numbering refers to *Streptomyces* sp N174 chitosanase **(B) Structure-based alignment of the conserved parts of the upper domain of the active site cleft from *Streptomyces* sp. N174 chitosanase and barley chitinase.** Structural elements established by crystallography are highlighted pale red, α-helices, violet, β-sheets, dark red, catalytic amino acids The Asp57 residue in the N174 chitosanase and the Asn124 residue in barley chitinase are shown in bold Structural data are from Refs. *7*, *16*, and *22*

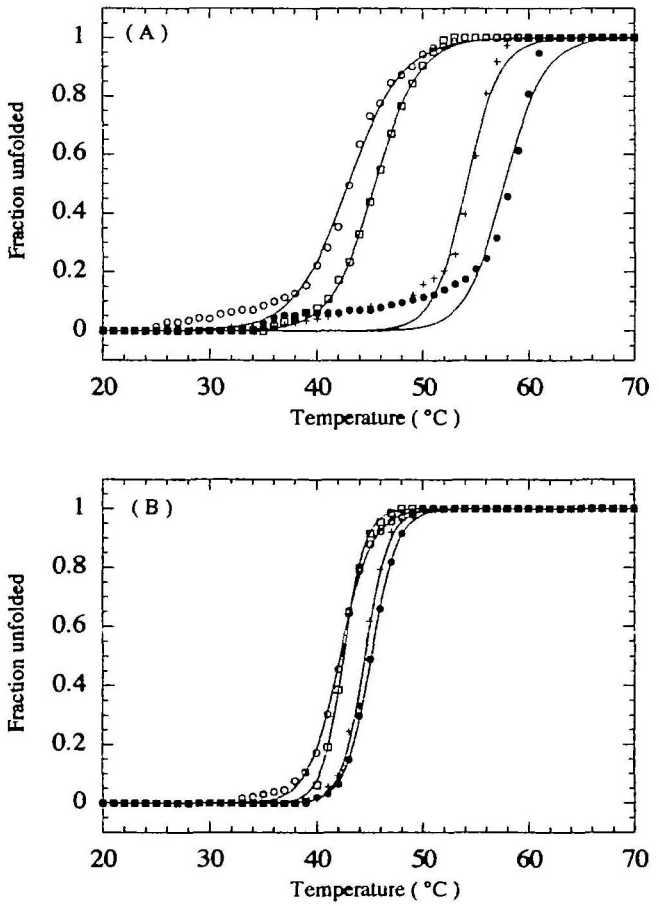

Fig 4 Thermal unfolding profiles of the E22Q (A) and D57A (B) mutant chitosanases obtained by monitoring CD at 222 nm. All unfolding curves were obtained in 50 mM sodium phosphate buffer, pH 7.0. The values of the thermodynamic parameters are listed in Table I ○, native enzyme; □, enzyme +$(GlcN)_3$, +, enzyme + $(GlcN)_6$, ●, enzyme + chitosan.

parameters could not be obtained because of strong substrate inhibition.

Chitosan Binding Ability of Chitosanases as Determined by Thermal Unfolding Experiments—For comparative purposes, we first examined the binding ability of the E22Q chitosanase in which the catalytic residue Glu22 is mutated to Gln. The hydrolytic activity of E22Q was known to be only 0 1% that of the wild type enzyme (*6*) We evaluated the substrate binding ability of this mutant by thermal unfolding, and found that the transition temperature (T_m) increased in the presence of $(GlcN)_n$ (Fig. 4A). The values of the thermodynamic parameters obtained from the unfolding curves are listed in Table I, and show that the stabilizing effect increases with increasing chain length of the added oligosaccharide. Similar experiments with the D57A chitosanase (Fig. 4B and Table I) revealed that protein stability was not enhanced upon the addition of $(GlcN)_3$. Furthermore, the enhancement of stability in D57A upon the addition of either $(GlcN)_6$ or short-chain highly-deacetylated chitosan (d.a. < 0.01, d.p. ≈ 20) was much less intense than that measured with E22Q. Control HPLC revealed only negligible hydrolysis of the saccharides added during the unfolding experiments. This suggests that the observed differences in unfolding behaviour between the E22Q and D57A chitosanases are due to a significant impairment of substrate binding with the D57A chitosanase. This experiment was not performed with the D57N mutant as it efficiently hydrolyses $(GlcN)_n$ substrates.

Hexasaccharide Digestion Experiments—When the wild type enzyme was incubated with $(GlcN)_6$, the substrate was almost completely degraded within 30 min (Fig. 5A), producing predominantly $(GlcN)_3$, although $(GlcN)_2$ and $(GlcN)_4$ were produced in smaller amounts. D57N completely hydrolysed $(GlcN)_6$ within 3 h, producing $(GlcN)_3$, $(GlcN)_2$, and $(GlcN)_4$ in a similar distribution to that of the wild type (Fig 6A). On the other hand, as much as 60 h was required for the complete digestion of $(GlcN)_6$ using an equivalent amount of D57A chitosanase (Fig. 7A). The product distribution produced by the D57A mutant was dif-

TABLE I **Thermodynamic parameters obtained from the thermal unfolding transition curves.**

Enzyme	T_m (°C)	ΔT_m (°C)	ΔH_m (kcal/mol)	ΔS_m (kcal/mol/°C)	$\Delta\Delta G_m$ (kcal/mol)
Wild type	42 3	0	115.5	0 37	
E22Q	42.9	0	78.4	0 25	0
E22Q+$(GlcN)_3$	45.4	2.5	97 0	0 30	0.63
E22Q+$(GlcN)_6$	54.2	11 3	134 4	0 41	2.83
E22Q+chitosan	57 7	14.8	116 7	0 35	3.70
D57A	42 2	0	134 0	0.43	0
D57A+$(GlcN)_3$	42 5	0 3	195 7	0.62	0 13
D57A+$(GlcN)_6$	44 5	2 3	181.1	0.57	0 99
D57A+chitosan	45 1	2 9	164.9	0 52	1 25

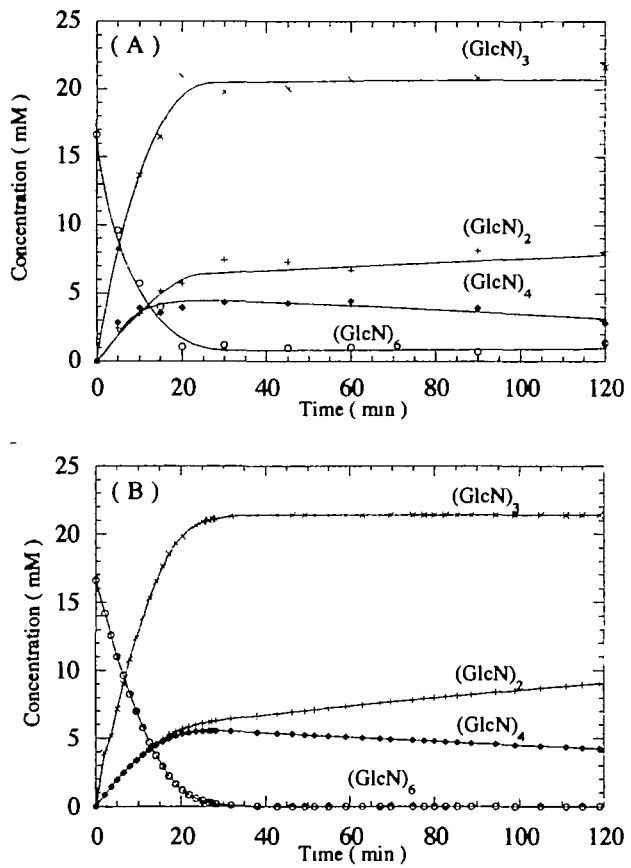

Fig. 5 **(A) Experimental reaction time-course of $(GlcN)_6$ degradation by the wild type chitosanase in 50 mM sodium acetate buffer, pH 5.0, at 40°C.** Enzyme concentration 0 37 μM. **(B) Theoretical reaction time course that best fits the experimental time course.** The constant values used for the calculation are listed in Table II

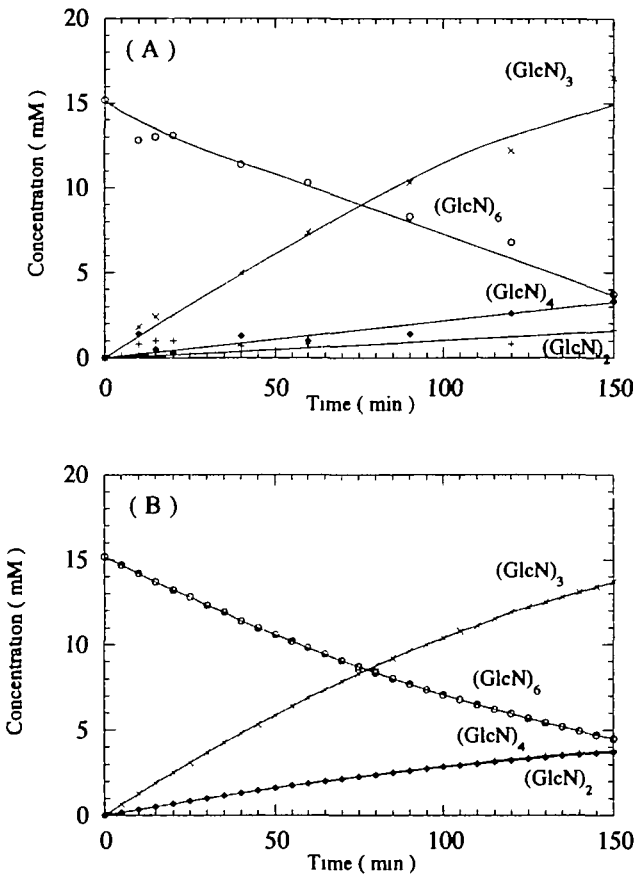

Fig 6 **(A) Experimental time-course of $(GlcN)_6$ degradation by the D57N mutant chitosanase in 50 mM sodium acetate buffer, pH 5.0, at 40°C.** Enzyme concentration 0 04 μM **(B) Theoretical time course that best fits the experimental time course.** The constant values used for the calculation are listed in Table II

ferent from that of the wild type enzyme, yielding smaller amounts of $(GlcN)_2$ and $(GlcN)_4$ as compared with the amount of $(GlcN)_3$ than did the wild type enzyme.

Theoretical Analysis of the Experimental Reaction Time-Course—Because of the structural similarity between barley chitinase and N174 chitosanase, the theoretical model used for the analysis of the barley chitinase reaction (*14*) was employed in the analysis of the chitosanase-catalyzed reaction. At first, the calculation was done with the binding free energy values obtained for barley chitinase, 0.0, –5.0, +4.1, –0.5, –3.8, and –2.0 kcal/mol for subsites (–3), (–2), (–1), (+1), (+2), and (+3), respectively. However, the product distribution of the calculated reaction time-course was much different from that obtained experimentally, and the degradation rate of the intermediate product $(GlcN)_4$ was higher in the calculated reaction time-course than in the experimental one. In order to control the product distribution, the free energy values of subsites (–3) and (+3) were changed to –0.5 and –1.0 kcal/mol, respectively. Next, the free energy values of subsites (–2) and (+2) were reduced to decrease the rate of $(GlcN)_4$ degradation. With –4.5 and –2.5 kcal/mol for subsites (–2) and (+2), the $(GlcN)_4$ degradation rate agreed with the experimental rate. Next, we tried to control the overall reaction rate by changing the free energy value of subsite (–1). The appropriate value was found to be +4.2 kcal/mol. Starting with these roughly esti-

mated values, optimization was conducted for the free energy values of the individual subsites. Finally, the value of the cost function attained the minimum when calculated with the values listed in Table II, and the reaction time-course calculated with these values is shown in Fig. 5B.

Fixing the rate constants at the values estimated for the wild type enzyme, optimization was conducted starting from the free energy values estimated for the wild type enzyme. In this case, however, only the values for subsites (–3), (–2), and (–1) were changed because the mutation of Asp57 does not affect the free energy values of the other subsites, which are located too far from the Asp57 residue in the chitosanase structure. Values of –0.7, –3.8, and +3.4 kcal/mol for subsites (–3), (–2), and (–1) were found to yield a minimum cost function (Table II), and the calculated best fit reaction time-course is shown in Fig. 6B.

Optimization of the reaction time-course obtained for the D57A mutant was conducted in a manner analogous to that for the D57N mutant. However, the value of the cost function did not decrease as much as in the case of the D57N mutant. The overall reaction rate of the calculated time-course was much higher than the experimental value. Therefore the optimization procedure was repeated using decreased k_1 values. With 5 s^{-1} for $(GlcN)_4$, 5 s^{-1} for $(GlcN)_5$, and 20 s^{-1} for $(GlcN)_6$, the fit between the experimental data and the calculated reaction time-course was satisfactory, and –1.7, 0.0, and +4.5 kcal/mol were deduced as the optimized values for subsites (–3), (–2), and (–1), respectively. The calculated, best fit reaction time-course is shown in Fig. 7B. The estimated rate constants and free energy values are listed in Table II.

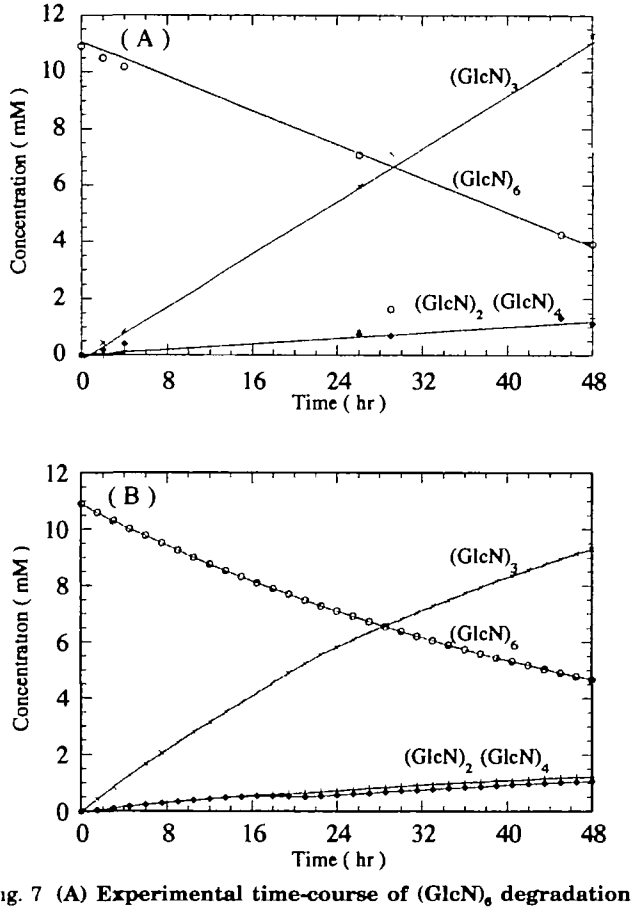

Fig. 7 **(A) Experimental time-course of $(GlcN)_6$ degradation by the D57A mutant chitosanase in 50 mM sodium acetate buffer, pH 5.0, at 40°C.** Enzyme concentration 0 25 μM. **(B) Theoretical time course that best fits the experimental time course.** The constant values used for the calculation are listed in Table II

DISCUSSION

Protein–carbohydrate interactions have been investigated using glycoside hydrolases resulting in the partial elucidation of their reaction mechanisms (*18*). Chemical modification and site-directed mutagenesis studies of lysozyme (*19*) have suggested a key role for tryptophan residues, because of both their ability to stack and their non-polar interaction with the pyranose ring of substrates. In the case of the interaction of chitosanase with its substrate, chitosan, the mechanism is thought to be significantly different Due to the polycationic character of chitosan, electrostatic interactions are believed to contribute significantly to substrate binding. If this is indeed the case, then carboxylic residues in chitosanase would be expected to play an important role in substrate binding

Not surprisingly, mutation of Asp57, a carboxylic residue located in a central position in the substrate binding cleft, significantly affects the enzymatic activity of chitosanase toward chitosan hexasaccharide. From thermal unfolding experiments and the theoretical analysis of the reaction time-course, this loss of activity was found to be due to a significant decrease in substrate binding ability at subsite (–2), indicating that Asp57 participates in substrate binding at this subsite. The fact that the substitution of the $-CH_2-COO^-$ in Asp57 with either $-CH_3$ (in D57A) or $-CH_2-CO-NH_2$ (in D57N) affects the substrate-binding activity suggests that the interaction of Asp57 with the substrate is electrostatic in nature and is eventually accompanied by hydrogen bonding. Marcotte *et al.* (*7*) suggested that there are two possible contacts between Asp57 and the sugar residue at subsite (–2); one is an electrostatic interaction with the sugar amine, and the other is a hydrogen bond with the hydroxyl oxygen at C3 of the pyranose ring Both interactions would be lost in the D57A mutant, while hydrogen bonding would be conserved in the D57N mutant. This

TABLE II **Kinetic parameters estimated from the theoretical calculation of the reaction time-course of hexasaccharide degradation using the reaction model shown in Fig. 1.**

Enzyme	k_1			k_2	Cleavage site ↓					
	$(GlcN)_4$	$(GlcN)_5$	$(GlcN)_6$		(–3)	(–2)	(–1)	(+1)	(+2)	(+3)
	(s^{-1})				(kcal/mol)					
Wild type ($-CH_2-COO^-$)	50	50	200	10,000	–0 7	–4 7	+4 2	–0 5	–2 3	–1.0
D57N ($-CH_2-CO-NH_2$)	350	350	1,400	10,000	–0.7	–2 0	+3.6	–0 5	–2.3	–1 0
D57A ($-CH_3$)	5	5	20	10,000	–1.7	0.0	+3 0	–0.5	–2.3	–1 0

explanation is consistent with the observed decrease in the free energy value at subsite (–2) (Table II).

Asp57 is located at the beginning of the third α-helix from the N-terminus of N174 chitosanase, and is just behind the third β-strand (Fig. 3). Superposition of secondary structural elements between chitinase, chitosanase, and lysozymes (*16*) suggests that Asp57 of chitosanase is located in a position equivalent to that of Trp62 in hen egg white lysozyme, a residue considered to be important in substrate binding by this enzyme (*19, 20*). The same comparison of the crystal structures (*16*) revealed that the position of Asp57 in N174 chitosanase is equivalent to that of Asn124 in barley chitinase (Fig. 3B). As reported earlier (*14*), among the six subsites of barley chitinase, subsite (–2) has the highest affinity for the GlcNAc residue, specifically –5.0 kcal/mol. From the crystal structure (*21*) and site-directed mutagenesis study of barley chitinase (*17*), Asn124 is considered to be one of the amino acids responsible for sugar binding at subsite (–2). Furthermore, Asn124 is located at the beginning of an α-helical structure corresponding to the third helix of N174 chitosanase. *Bacillus circulans* MH-K1 chitosanase also has an aspartic acid residue at a position corresponding to Asp57 of N174 chitosanase (*22*). Together these observations strongly support the idea that Asp57 is one of the amino acids responsible for substrate binding in *Streptomyces* sp. N174 chitosanase.

As described above, steady state kinetic parameters of the enzymes could not be obtained because of their strong substrate inhibition To obtain the kinetic constants, therefore, we analyzed the reaction time-course of hexasaccharide degradation on the basis of the subsite theory, in which the binding free energy change of oligosaccharide binding is assumed to be equal to the sum of the values for the individual subsites occupied by the substrate sugar residues (additivity). In the classical model of subsite enzymes, it is further assumed that the rate constant values and binding free energy changes are independent of substrate occupancy in the binding cleft (*23*). Today, however, such an assumption is not acceptable, because it is likely that substrate occupancy cooperatively affects the catalytic constant and binding free energy of the enzyme. In our time-course analysis, the rate constant of bond-cleavage (k_1) is assumed to be dependent upon the size of the substrate. From the product distribution obtained for the oligosaccharide substrates [$(GlcN)_{4-6}$], it was confirmed that $(GlcN)_6$, $(GlcN)_5$, and $(GlcN)_4$ bind to (–3)–(+3), (–2)–(+3) or (–3)–(+2), and (–2)–(+2), respectively (*24*). Thus, the substrate size dependence of the rate constant of bond cleavage can be regarded as an alternative to the substrate occupancy dependence. In fact, the subsite enzyme model that included substrate size dependence resulted in a satisfactory fit between the experimental and theoretical time-courses (Figs. 5–7) We believe that, at present, the model employed in this study is the most appropriate for kinetic analysis of N174 chitosanase.

Analysis of the reaction time-course of $(GlcN)_6$ cleavage by N174 chitosanase led to the conclusion that the productive binding of $(GlcN)_6$ to the enzyme is better described by a symmetrical model including subsites (–3)(–2)(–1)(+1)(+2)(+3), with cleavage occuring in the middle. This is analogous to a model previously deduced for barley chitinase and goose egg white lysozyme (*14*), and is consistent with the early observation that the trimer is by far the most abundant product obtained from the hydrolysis of $(GlcN)_6$ by N174 chitosanase (*24*). This is somewhat in contrast to the substrate binding models for chitosanases based on the adaptation of the lysozyme paradigm (*7, 22*) in which an interaction of the enzyme with the sugar residue at subsite (+3) is not included. However, these non-symmetrical binding models were based on the structures of chitosanase crystals with no bound substrate. Such chitosanase crystals have a rather open structure as illustrated by the fact that the distance between the oxygen atoms of the catalytic residues (Glu22 and Asp40) observed in chitosanase crystals (11–14 Å) is significantly longer than the average for glycosyl hydrolases with an inverting mechanism (9.5 Å; *25*). In these open structures, no residues with the potential to interact with the sugar at the (+3) subsite could be determined. Consequently, it is postulated that chitosanases undergo a substantial structural rearrangement while binding to substrate.

In conclusion, Asp57 of *Streptomyces* sp. N174 chitosanase participates in the binding of the sugar residue at subsite (–2), most probably through both electrostatic and hydrogen bonding interactions. Although the hexasaccharide substrate mainly binds to the entire binding cleft, (–3)(–2)(–1)(+1)(+2)(+3), of the chitosanase, the Asp57 interaction with the sugar residue at subsite (–2) is the most important for the binding of chitosan oligosaccharide to chitosanase.

We are grateful to Dr K.M. Vårum, Norwegian University of Science and Technology, for kindly supplying the low d a. chitosan and to William Home for reviewing the manuscript

REFERENCES

1 Fukamizo, T, Ohkawa, T, Ikeda, Y, and Goto, S (1994) Specificity of chitosanase from *Bacillus pumilus*. *Biochim. Biophys. Acta* **1205**, 183–188
2 Mitsutomi, M, Kidoh, H., Tomita, H, and Watanabe, T. (1995) The action of *Bacillus circulans* WL-12 chitinases on partially *N*-acetylated chitosan *Biosci. Biotechnol Biochem* **59**, 529–531
3 Ohno, T., Armand, S, Hata, T, Nikaidou, N, Henrissat, B, Mitsutomi, M, and Watanabe, T (1996) A modular family 19 chitinase found in the prokaryotic organism *Streptomyces griseus* HUT 6037 *J Bacteriol* **178**, 5065–5070
4. Vårum, K.M, Holme, H K., Izume, M, Stokke, B T, and Smidsrød, O (1996) Determination of enzymatic hydrolysis specificity of partially N-acetylated chitosans *Biochim Biophys. Acta* **1291**, 5–15
5 Fukamizo, T and Brzezinski, R (1997) Chitosanase from *Streptomyces* sp strain N174 a comparative review of its structure and function *Biochem Cell Biol* **75**, 687–696
6 Boucher, I, Fukamizo, T, Honda, Y., Willick, G E, Neugebauer, W.A., and Brzezinski, R. (1995) Site-directed mutagenesis of evolutionary conserved carboxylic amino acids in the chitosanase from *Streptomyces* sp N174 reveals two residues essential for catalysis. *J Biol Chem.* **270**, 31077–31082
7 Marcotte, E M, Monzingo, A.F, Ernst, S R, Brzezinski, R, and Robertus, J D (1996) X-ray structure of an anti-fungal chitosanase from *Streptomyces* N174. *Nat Struct Biol.* **3**, 155–162
8 Kelly, J A., Sielecki, A.R., Sykes, B D., James, M.N G., and Phillips, D C. (1979) X-ray crystallography of the binding of the bacterial cell wall trisaccharide NAM-NAG-NAM to lysozyme. *Nature* **282**, 875–878
9 Hopwood, D.A., Bibb, M.J., Chater, K.F, Kieser, T., Bruton, C.J, Kieser, H M, Lydiate, D.J, Smith, C.P, Ward, J.M, and Schrempf, H (1985) *Genetic Manipulation of Streptomyces: a Laboratory Manual*, The John Innes Foundation, Norwich,

England
10 Denis, F. and Brzezinski, R. (1992) A versatile shuttle cosmid vector for use in *Escherichia coli* and actinomycetes *Gene* **111**, 115–118
11. Masson, J-Y., Li, T, Boucher, I., Beaulieu, C, and Brzezinski, R. (1993) Factors governing an efficient chitosanase production by recombinant *Streptomyces lividans* strains carrying the cloned chs gene from *Streptomyces* sp N174 in *Chitin Enzymology* (Muzzarelli, R.A.A., ed) pp 423–430, European Chitin Society, Ancona
12. Lever, M. (1972) A new reaction for colorimetric determination of carbohydrates. *Anal. Biochem* **47**, 273–279
13. Becktel, W.J and Schellman, J.A (1987) Protein stability curves. *Biopolymers* **26**, 1859–1877
14. Honda, Y. and Fukamizo, T (1998) Substrate binding subsites of chitinase from barley seeds and lysozyme from goose egg white *Biochim Biophys. Acta* **1388**, 53–65
15 Kuhara, S, Ezaki, E., Fukamizo, T., and Hayashi, K. (1982) Estimation of the free energy change of substrate binding lysozyme-catalyzed reactions. *J Biochem.* **92**, 121–127
16 Monzingo, A.F, Marcotte, E M., Hart, P J, and Robertus, J D (1996) Chitinases, chitosanases, and lysozymes can be divided into procaryotic and eucaryotic families sharing a conserved core *Nat Struct. Biol* **3**, 133–140
17 Andersen, M.D., Jensen, A., Robertus, J D, Leah, R., and Skriver, K. (1997) Heterologous expression and characterization of wild-type and mutant forms of a 26 kDa endochitinase from barley (*Hordeum vulgare* L) *Biochem. J* **322**, 815–822
18. Vyas, N K. (1991) Atomic features of protein-carbohydrate interactions. *Curr Opin Struct Biol* **1**, 732–740
19. Maenaka, K., Kawai, G., Watanabe, F, Sunada, F, and Kumagai, I (1994) Functional and structural role of a tryptophan generally observed in protein-carbohydrate interaction Trp-62 of hen egg white lysozyme *J Biol Chem.* **269**, 7070–7075
20 Fukamizo, T, Kuhara, S, and Hayashi, K. (1982) Enzymatic activity of Trp 62-modified lysozyme *J. Biochem.* **92**, 717–724
21. Hart, P J., Pfluger, H D, Monzingo, A F., Hollis, T., and Robertus, J D. (1995) The refined crystal structure of an endochitinase from *Hordeum vulgare* L seeds at 1.8 Å resolution *J Mol. Biol* **248**, 402–413
22 Saito, J-I., Kita, A., Higuchi, Y, Nagata, Y, Ando, A., and Miki, K. (1999) Crystal structure of chitosanase from *Bacillus circulans* MH-K1 at 1 6-Å resolution and its substrate recognition mechanism *J Biol Chem* **274**, 30818–30825
23 Masaki, A., Fukamizo, T., Ohtakara, A., Torikata, T, Hayashi, K., and Imoto, T (1981) Estimation of rate constants of lysozyme-catalyzed reaction of chitooligosaccharides *J Biochem* **90**, 1167–1175
24. Fukamizo, T., Honda, Y, Goto, S, Boucher, I., and Brzezinski, R. (1995) Reaction mechanism of chitosanase from *Streptomyces* sp N174. *Biochem. J* **311**, 377–383
25. Wang, Q., Graham, R W, Trimbur, D, Warren, R.A.J, and Withers, S.G. (1994) Changing enzymatic reaction mechanism by mutagenesis conversion of a retaining glucosidase to an inverting enzyme *J. Am. Chem. Soc.* **116**, 11594–11595